

Towards a spectroscopically accurate set of potentials for heavy hydride laser cooling candidates: effective core potential calculations of BaH

Keith Moore, Brendan M. McLaughlin, and Ian C. Lane^{a)}

School of Chemistry and Chemical Engineering, Queen's University Belfast, Stranmillis Road, Belfast BT9 5AG, UK

(Dated: 1 March 2022)

BaH (and its isotopomers) is an attractive molecular candidate for laser cooling to ultracold temperatures and a potential precursor for the production of ultracold gases of hydrogen and deuterium. The theoretical challenge is to simulate the laser cooling cycle as reliably as possible and this paper addresses the generation of a highly accurate *ab initio* $^2\Sigma^+$ potential for such studies. The performance of various basis sets within the multi-reference configuration-interaction (MRCI) approximation with the Davidson correction (MRCI+Q) is tested and taken to the Complete Basis Set (CBS) limit. It is shown that the calculated molecular constants using a 46 electron Effective Core-Potential (ECP) and even-tempered augmented polarized core-valence basis sets (aug-pCV n Z-PP, $n = 4$ and 5) but only including three active electrons in the MRCI calculation are in excellent agreement with the available experimental values. The predicted dissociation energy D_e for the $X^2\Sigma^+$ state (extrapolated to the CBS limit) is 16895.12 cm^{-1} (2.094 eV), which agrees within 0.1% of a revised experimental value of $<16910.6 \text{ cm}^{-1}$, while the calculated r_e is within 0.03 pm of the experimental result.

I. INTRODUCTION

Recently, it has been proposed¹ that ultracold hydrogen atoms may be formed by the photo-dissociation of laser cooled hydrides, provided the energy of the fragmentation products is much smaller than the average thermal energy of the parents. At the limit of zero kinetic energy release, the velocities of the hydrogen atoms will match that of the parents, forming a Maxwellian velocity distribution corresponding to a much lower hydrogen atom temperature than the original molecular gas ($T_H = \frac{T_{MH}}{m_{MH}}$). Quantum chemical calculations of the transition dipoles and Franck-Condon (FC) factors, using the post Hartree-Fock methods Complete Active Space Self Consistent Field (CASSCF)² and MRCI³, confirmed that BaH was a very good candidate for demonstrating this kinematic effect as the barium atom has a considerable mass and the molecular radical is amenable to laser cooling⁴. In the earlier study a very small (triple zeta quality) two electron basis set for barium was used with the inner 52 electrons replaced by an ECP. To improve agreement with the experimental energy levels of the atom, an ℓ -independent Core-Polarization Potential (CPP) was added to the calculation. Although the resulting basis set simulated the reported experimental FC factors very well, there were clearly issues with the calculation of the ground state equilibrium bond length r_e (experimental value⁵ $2.23188651(19) \text{ \AA}$) and the dissociation limit⁶⁻⁹. This paper attempts to produce a global, high-quality *ab initio* potential for the $X^2\Sigma^+$ ground state of BaH. The heavier familial hydrides YbH and RaH are also attractive precursors of ultracold hydrogen but, unlike BaH, there is currently a lack of reliable theoretical or

experimental data to confirm their suitability. Hydrogen forms the basis of many spectroscopic tests of fundamental symmetries¹⁰, for the evolution of the Universe¹¹ and in metrology^{12,13} (for example, the measurement of the Rydberg constant¹⁴ and the proton radius¹⁵).

BaH is naturally a heavier cousin of BeH, the simplest stable neutral open shell diatomic. BeH possesses just five electrons and has recently been the focus of two important papers^{16,17} regarding the simulation of its ground potential energy curve. The first¹⁶ was a detailed *ab initio* study using very large correlation consistent basis sets (aug-cc-pCV n Z) up to seven zeta ($n = 7$) in character (indeed so large that the MOLPRO¹⁸ *ab initio* package could not use the largest $\ell = 7$ functions in the basis set and the effect of excluding them was determined by a separate calculation). When determining the static electron correlation beyond Hartree-Fock level, the CASSCF wavefunction included the excited $3s$ and $3p$ orbitals on the Be atom within the active space despite this being a single electronic state calculation. To avoid the size-extensivity issues inherent in MRCI (for dynamic electron correlation) the MR-ACPF¹⁹ (multi-reference averaged coupled-pair functional) method was used instead. The size-extensivity and basis set superposition errors (BSSE) were determined to both be around $1\text{-}2 \text{ cm}^{-1}$ at the $n = 7$ level of calculation. The calculations were then extrapolated to the CBS limit. Despite the meticulous care taken in producing this *ab initio* potential, the resulting equilibrium bond length deviated by 0.13 pm from the spectroscopic value. While in excellent agreement for a typical *ab initio* calculation, for a benchmark molecule it is a little disappointing that such a powerful calculation could not achieve a better agreement. Tremendous pains were then made¹⁶ to include a host of minor corrections to the potential including electron correlation beyond the MR-ACPF method (to a level equivalent to full CI), scalar relativistic effects and diagonal Born-

^{a)}Electronic mail: i.lane@qub.ac.uk

Oppenheimer corrections (DBOC). However, the energy effect of each of these additional contributions (all calculated using much smaller basis sets than used in the MRCI calculation) was small and mutually cancelling, while the improvement in bond length was just 0.04 pm. Furthermore, the bond dissociation energy was 90 cm^{-1} higher than the best experimental data²⁰ at that point ($17590 \pm 200 \text{ cm}^{-1}$), though smaller than the raw *ab initio* result (17699 cm^{-1}). The second paper¹⁷ concerned taking that experimental work by Le Roy *et al*²⁰ and fitting a new analytical function to the spectroscopic data. Just 5% of the rotationless adiabatic potential has yet to be covered experimentally and still the quantum number of the highest bound vibrational state is unclear. Again great attention to detail was conducted in this study, including mass corrected C_6 , C_8 and C_{10} constants for the different hydrogen isotopes. Despite this, the question of whether $v = 12$ is the highest vibrational level is still unresolved but the experimental D_e is now within 1 cm^{-1} of the corrected *ab initio* value. If confirmed by future experiments, this would be an amazing achievement for *ab initio* quantum chemistry.

Given the difficulties in describing the relatively simple BeH, the task of completing accurate potentials for the heavier system BaH, that contains an additional 52 electrons, looks formidable. Furthermore, relativistic effects that were tiny in BeH are amplified in such a heavy hydride. However, 46 or even 54 of the electrons can be replaced with an ECP and many of the scalar relativistic effects can be included in that potential. The larger core was used by Lane¹ and earlier by Preuss and co-workers⁶ but in both instances the predicted ground state bond length was calculated to be much too short using a triple zeta basis set. While Preuss and co-workers^{6,7} managed to achieve 1 pm accuracy using a smaller ($4s,4p,2d$) basis set, such behavior is symptomatic of simple error correction. Furthermore, both D_e and ω_e were much lower⁶ than experimental estimates at that time. It should not be forgotten that, despite the short bond length, the 2-electron, CPP + ECP calculation of FC factors is sufficiently accurate¹ to be useful for screening good laser cooling transitions. For accurate calculation of the molecular constants, however, the evidence points to a minimum ten-electron basis set for barium.

Adopting the smaller 46-electron ECP allows the introduction of core-valence interactions with the $5s$ and $5p$ electrons as well as providing an opportunity to adjust the number of electrons used in calculating static and dynamic electron correlation. The change in ECP increased the predicted r_e value of Kaupp *et al*⁷ by a further 10 pm but this value was now 4 pm too high. Going one step further, Allouche *et al*⁸ introduced an ℓ -dependent CPP into a CI calculation of the lowest electronic states of BaH using a triple zeta basis set. Although there were eleven valence electrons, only three were active in the CI step. The $X^2\Sigma^+$ state equilibrium bond length was still 3 pm too large, but the agreement is better than Kaupp *et al*.⁷ In addition the molecular constants for all

the excited states correlating the lowest five electronic states of barium were calculated. They also investigated the effect of including spin-orbit coupling in the computation and demonstrated it made no difference (at the 100 fm level) to the ground state bond length and altered excited states by $< 0.3 \text{ pm}$. However, the spin-orbit model adopted was fairly basic and consequently the spin-orbit constants were up to 60% too large. The calculated dissociation energy, D_e , of 2.04 eV was significantly larger than the earlier value of 1.79 eV recommended by Fuentealba⁶ *et al* from their pseudo-potential plus single and double configuration interactive (CISD) model, with an equilibrium bond distance of 2.3707 Å. We note that Fuentealba *et al*⁶ also obtained a value of 2.1 eV for D_e using a pseudo-potential plus local spin density (LSD) approximation with an equilibrium bond distance of 2.4829 Å. That dissociation energy is in excellent agreement with a recent relativistic coupled-cluster (RCCSDT) value of 2.062 eV by Skripnikov *et al*⁹. This is interesting in itself as such agreement between relativistic and essentially non-relativistic calculations is rather unexpected in such a heavy hydride. Despite the close agreement between the highlighted theoretical bond energies, they are all larger than the accepted²¹ experimental value.

Following its discovery in the visible emission spectra²² of the Group II hydrides by Eagle in 1909 the $E^2\Pi \rightarrow X^2\Sigma^+$ $0-0$ band in BaH was assigned by Schaafsma²³ around the time that Watson began a series of spectroscopic studies on BaH recording²⁴ the (1 - 1) and (2 - 2) $E^2\Pi \rightarrow X^2\Sigma^+$ emission bands (Funke later²⁵ added the non-diagonal (0 - 1) and (2 - 1) bands). Watson followed that work with the first spectra of the $B^2\Sigma^+ \rightarrow X^2\Sigma^+$ transition²⁶ in the near infra-red, which revealed an exceptionally large value for the spin-rotation constant in the upper state. As this constant was determined to be negative, it suggested the presence of the lower lying $A^2\Pi$ state that was formally identified by the group^{27,28} two years later. Also conjectured in these papers was the presence²⁷ of an even lower lying excited $^2\Delta$ state, though this $H^2\Delta$ potential was finally directly observed²⁹ by Fabre *et al*. only in 1987. In 1936 Grunström³⁰ reported a new higher lying electronic state and analysed the (0 - 0) and (0 - 1) bands of this violet $C^2\Sigma^+ \rightarrow X^2\Sigma^+$ transition, a similar band having been observed in lighter Group II hydrides. Further investigation³¹ revealed that the $v' = 1$ level is abruptly predissociated above $N = 10$ and it was speculated there was a lower bound state with an extended equilibrium bond length.

A series of papers in the 1960s by Kopp and colleagues revealed absorptions in the UV³², identified the $D^2\Sigma^+$ state²¹ perturbing the $C^2\Sigma^+$ vibronic structure, recorded the $B^2\Sigma^+ \leftarrow X^2\Sigma^+$ transition in BaD³³ and added additional vibrational levels to the $A^2\Pi \leftarrow X^2\Sigma^+$ absorption spectra³⁴ for both hydrogen isotopes. However, due to the highly diagonal transitions in the $A^2\Pi$, $B^2\Sigma^+$ and $C^2\Sigma^+ \leftarrow X^2\Sigma^+$ absorption bands, direct observations of vibrational levels were limited to $v = 0 - 2$ for all the

electronic states involved. Only the $D^2\Sigma^+$ state had a potential minimum significantly displaced from that of the ground state but has only been studied in absorption so while the $D^2\Sigma^+$ state has been studied up to $v = 9$, the ground state remains unexplored^{5,35} above $v = 3$. Furthermore, the often quoted experimental value for the dissociation energy in the ground state, $D_e < 16350 \text{ cm}^{-1}$, is based²¹ on the analysis of predissociation in the $C^2\Sigma^+$ state and assumptions made about the nature of mechanism involved.

II. AB INITIO CALCULATIONS

A. Computational methods

The initial results reported here were obtained using a parallel version of the MOLPRO¹⁸ suite of *ab initio* quantum chemistry codes (release MOLPRO 2010.1). MRCI calculations based on State-Averaged Multi-Configuration-Self-Consistent-Field (SA-MCSCF) wavefunctions^{2,36,37} were conducted to determine the potential energy curves as a function of internuclear distance r out to bond separation of $r = 40 \text{ bohr}$ (a_0). When dealing with dissociating systems, size-consistency in the calculation is a particular concern, particularly with CI methods³⁸ restricted to single and double excitations such as the MRCI code in MOLPRO. To estimate the missing higher excitations, the *a posteriori* Davidson correction³⁹ was applied to all the results (MRCI + Q). To model the molecular orbitals a variety of correlation-consistent Gaussian basis sets⁴⁰ were trialled; aug-cc-pVnZ, cc-pCVnZ-PP, cc-pwCVnZ-PP and aug-cc-pCVnZ-PP. In each calculation, the 46 core electrons of the barium atom were described with an effective core potential of the form ECP46MDF from the Stuttgart group⁴¹ leaving the outer ten 5s5p6s electrons. This allows one to test how each basis set performs for the molecular constants, e.g.; the equilibrium bond length and the dissociation energy D_e while keeping the active space constant.

All the electronic structure computations are performed in the C_{2v} Abelian point group symmetry. In the C_{2v} point group, molecular orbitals are labelled according to symmetries a_1, b_1, b_2 and a_2 ; when the molecular symmetry is reduced from $C_{\infty v}$ to C_{2v} , the correlating relationships are $\sigma \rightarrow a_1$, $\pi \rightarrow (b_1, b_2)$, $\delta \rightarrow (a_1, a_2)$. The preferred active space consists of 11 electrons and 17 molecular orbitals $7a_1, 5b_1, 3b_2, 2a_2$; i.e. a (7,5,3,2) model. However, to describe the Rydberg character of the highly excited states of A_1 symmetry it was necessary sometimes to expand the active space to $(9a_1, 5b_1, 3b_2, 2a_2)$. The averaging process was carried out on the lowest five $^2\Sigma^+$, $^2\Pi$ and $^2\Delta$ molecular states of this hydride.

B. Ab initio potentials using an AV6Z basis

Typically, the basis set of choice for an MRCI + Q calculation including excited electronic states is the augmented correlation consistent type such as aug-cc-pVnZ to provide the diffuse Gaussians required to model the higher energy electron orbitals. In addition, the larger the value of n the more faithful the model wavefunctions match the real ones. Therefore, the first computations on this hydride were performed using an aug-cc-pV6Z basis on both atoms (Fig. 1), extending the previous work of Lane¹. The calculated potentials can be grouped according to three broad types:

- (1) Bound potentials based on the interaction between a Ba^+ cation and H^- anion e.g. the $X^2\Sigma^+$ and $A^2\Pi$ states,
- (2) Rydberg states with a single electron held within the potential of a BaH^+ molecular ion composed of Ba^{2+} and H^- ions e.g. $C^2\Sigma^+$ and
- (3) extended bond length states formed by the avoided crossing of largely repulsive valence curves and attractive ionic potentials e.g. $D^2\Sigma^+$.

Only doublet states were investigated as the lowest quartet states⁸ are all repulsive. The historical spectroscopic assignments were used for the electronic states in Fig. 1 although it is clear that the adiabatic $3^2\Sigma^+$ potential is reported as two separate states experimentally ($C^2\Sigma^+$ and $D^2\Sigma^+$). The calculated energy gaps at the majority of the avoided crossings in BaH are tiny (the case of the $2^2\Sigma^+ - X^2\Sigma^+$ diabats being a noteworthy exception) and consistent with experiments where, for example, the Rydberg $C^2\Sigma^+$ vibrational progression²¹ is maintained for energies well above that of the C/ $D^2\Sigma^+$ states' closest approach (inset, Fig. 1). These AV6Z $\Lambda\Sigma$ potentials are consistent with previous work by Allouche⁸ *et al.*

For the ground $X^2\Sigma^+$ state the calculated value of $r_e = 2.18 \text{ \AA}$ is in close agreement to the value of $r_e = 2.16 \text{ \AA}$ obtained¹ using a barium triple zeta basis set (cc-pV5Z basis on the hydrogen), a 56-electron ECP and an ℓ independent core polarisation potential (CPP). However, the accepted experimental value⁵ for r_e is 2.2319 \AA . The AV6Z basis set also predicts a dissociation energy D_e of 2.2687 eV (18293.08 cm^{-1}) while the experimental value reported by Kopp *et al.*²¹ is considerably smaller, $< 2.0271 \text{ eV}$ (16350 cm^{-1}). Both the discrepancies in the equilibrium bond length and the dissociation energy are rather large for an MRCI+Q calculation with such a substantial barium basis set. Therefore, the investigation was widened to include a variety of other basis sets in an attempt to improve the agreement between the *ab initio* results for the ground state for this hydride and the spectroscopic constants.

C. Augmented basis sets

An even tempered augmentation can be used to extend both the cc-pCVQZ-PP and the cc-pCV5Z-PP basis⁴⁰

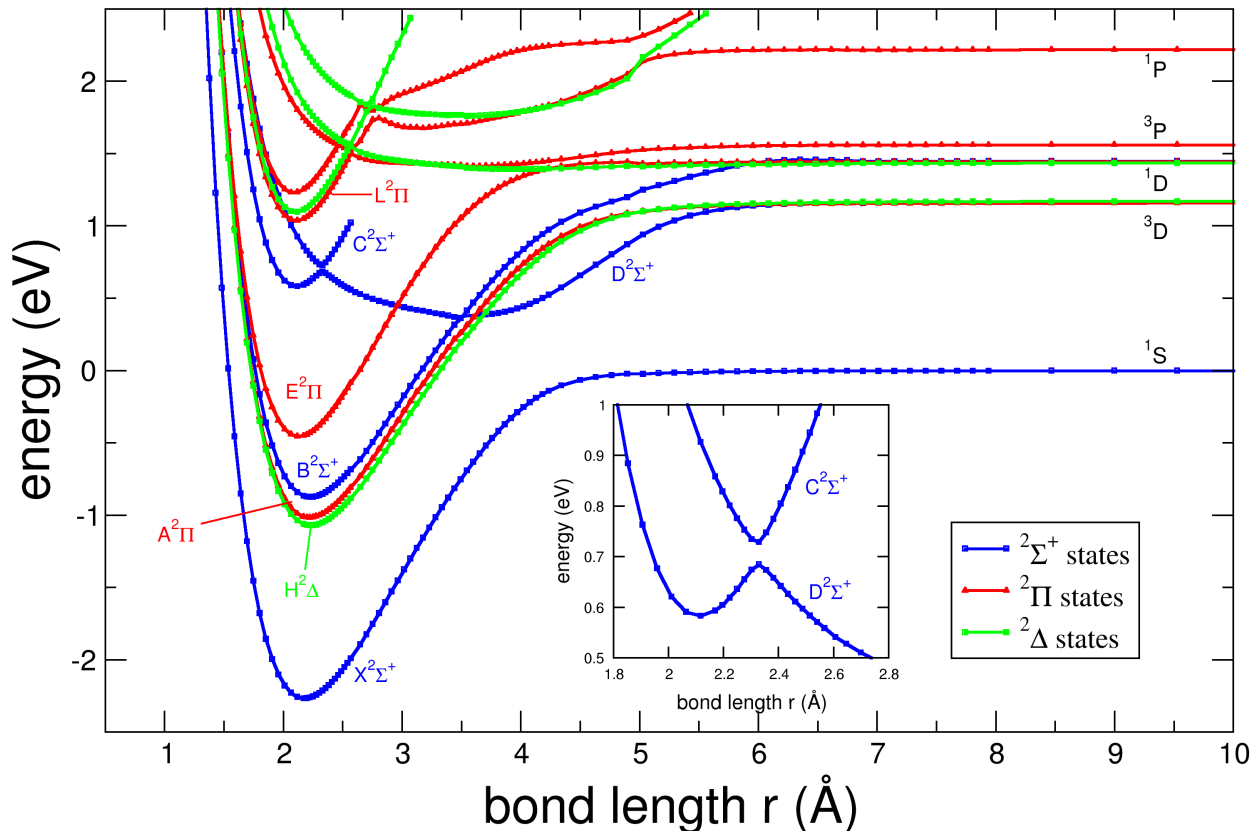


FIG. 1. MRCI+Q results for the lowest 5 states of each symmetry ($^2\Sigma^+$, $^2\Pi$ and $^2\Delta$) as a function of bond length. The calculations have been performed with an aug-cc-pV6Z basis set and an ECP with the MOLPRO suite. The potentials shown were used to extract values for both the equilibrium bond distance r_e and dissociation energy D_e . For the ground $X^2\Sigma^+$ state, the calculated equilibrium bond length is $r_e=2.18$ Å while the dissociation energy is $D_e = 2.2687$ eV. The electronic states of the Ba atom fragments are also labelled (only H atoms in the lowest 1^2S state are produced at these energies). Inset: details of the avoided crossing between C/D $^2\Sigma^+$ states.

sets. Each basis set is augmented with a single diffuse Gaussian function, the augmented exponent α' given by the expression,

$$\alpha'(\ell) = \frac{\alpha^2(\ell)}{\beta(\ell)} \quad (1)$$

where $\alpha(\ell)$ and $\beta(\ell)$ are respectively the last and second last exponent of the appropriate basis set. Calculations are performed in the MRCI+ Q approximation for the even tempered augmented sets (the additional functions are presented in Table I) and explicitly optimized augmented cc-pCVnZ-PP ($n = 4$ and 5) sets⁴⁰ (these explicitly optimized functions are presented in Table II). A large augmented basis set is chosen because in quantum chemistry calculations they are known to recover typically ~ 99 % or more of the electron correlation energy.

D. CCSD(T) versus MRCI+Q

In the search for an ideal basis set, numerous calculations with the MOLPRO suite were performed for the ground state of this hydride. Table III presents results for the different basis sets used in the MRCI+Q approximation, both for the equilibrium bond distance r_e and dissociation energy D_e , and compares them to CCSD(T) calculations⁴⁰ on BaH. CCSD(T) is currently regarded as the most reliable theoretical method for information on ground state potentials. In the MRCI+Q calculations, the CASSCF step is performed over the lowest three 2A_1 , 2B_1 , and 2A_2 states while only the lowest

TABLE I. Augmented functions to the $cc\text{-pCV}n\text{Z-PP}$ basis set⁴⁰ for barium. The even tempered augmentation procedure is used, where $\alpha(\ell)$ and $\beta(\ell)$ are respectively the last and second last exponent in appropriate basis set.

$cc\text{-pCVQZ-PP}$		Barium
Angular momentum function		Exponent ^a
s		0.32620
p		0.10943
d		0.18940
f		0.43550
g		0.47145
$cc\text{-pCV5Z-PP}$		Barium
Angular momentum function		Exponent ^a
s		0.18570
p		0.11590
d		0.29510
f		0.38060
g		0.46480
h		0.62250

^aEstimated using $\alpha'(\ell) = \frac{\alpha^2(\ell)}{\beta(\ell)}$

TABLE II. Augmented functions to the $cc\text{-pCV}n\text{Z-PP}$ basis set for barium. For the augmentation procedure the exponents are optimised⁴⁰ on the energy of the ground state of the BaH molecule.

$cc\text{-pCVQZ-PP}$		Barium
Angular momentum function		Exponent
s		0.0073
p		0.0060
d		0.0114
f		0.0373
g		0.0492
$cc\text{-pCV5Z-PP}$		Barium
Angular momentum function		Exponent
s		0.0071
p		0.0058
d		0.0089
f		0.0326
g		0.0393
h		0.0515

² A_1 state appears in the MRCI code. It appears that the even tempered augmented basis set $aug\text{-}cc\text{-pCV5Z-PP}$ performs best at MRCI+Q level for the ground state, matching within 0.1pm the experimental r_e value. The explicitly optimized augmented basis set $aug\text{-pCV5Z-PP}$ gives comparable equilibrium bond distances. In contrast to calculations using CCSD(T), the $cc\text{-pCV}n\text{Z-PP}$ basis sets pull the equilibrium bond lengths to much shorter values when using the MRCI + Q method. Augmenting the basis set with diffuse orbitals helps to counteract this effect. From Table III the CCSD(T), all electron, work⁴⁰

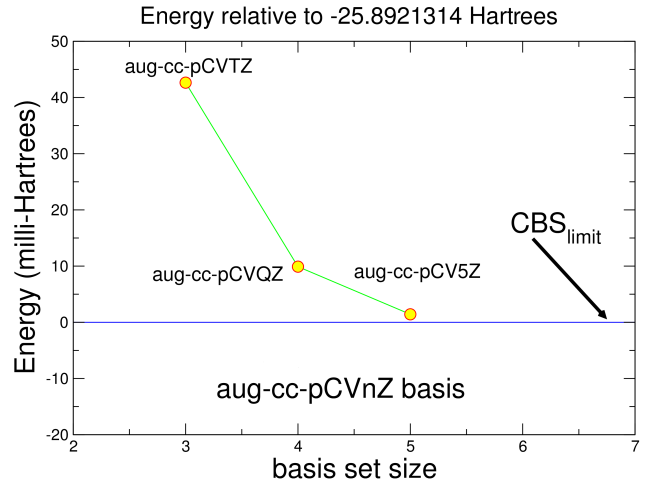


FIG. 2. BaH minimum energy in $X \ ^2\Sigma^+$ state, the approach to the CBS limit using an active 3-electron model in the MRCI+Q approximation. Even tempered $aug\text{-}cc\text{-pCV}n\text{Z-PP}$ basis sets are used in the calculations.

provides results (with either the $cc\text{-pCV5Z-PP}$ or $cc\text{-pwCV5Z-PP}$ basis) comparable to the present MRCI+Q results with the even tempered augmented basis set. The MRCI + Q calculations are also in excellent agreement with the previous RCCSDT⁹ and MRCI+Q + including spin-orbital coupling (SOC)⁴² values for the dissociation energy. In addition, this optimal basis set can also be used to carry out calculations of excited states, such as $A^2\Pi$, a significant advantage of the MRCI method over CCSD(T).

E. Complete Basis Set Limit

To remove the uncertainty that any close agreement with experiment is the result of computational artefacts, it is best to extrapolate the energies E_n calculated with the VnZ basis sets to the limit of an infinite number of Gaussian functions. For the various basis sets shown in Table III the potential energy of the ground state via the complete basis set limit (CBS) is found using the formulae derived by Jensen⁴³ with modifications by Karton and Martin⁴⁴

$$E_{CBS} = E_n + \frac{(E_n - E_{n-1})}{\frac{n}{n+1} \exp[9(\sqrt{n} - \sqrt{n-1}) - 1]} \quad (2)$$

where here $n = 5$. This expression is used to determine all the CBS potential energy curves in this study. Fig 2 shows the orderly approach to the CBS energy limit for the even tempered augmentation of the $cc\text{-pCV}n\text{Z-PP}$ basis⁴⁰ set. While this extrapolation is usually adopted for static-correlation only, the small dynamic correlation found in the BaH calculations prompted its use here. The

TABLE III. Spectroscopic constants for the $X^2\Sigma^+$ ground state of the BaH molecule: the equilibrium bond distance r_e (Å) and the dissociation energies D_e in eV and cm^{-1} . Comparison of the present MRCI + Q results with a variety of other reported values using correlation - consistent basis sets⁴⁰ (cc-pVnZ-PP, aug-cc-pVnZ-PP, cc-pCVnZ-PP, cc-pwCVnZ-PP, and aug-cc-pCVnZ-PP), both with CI and CCSDT methods (fc, is frozen core, all, is all-electron) and other previous theoretical work. The best experimental values are also included.

Basis	Method	r_e (Å)	D_e (eV)	D_e (cm^{-1})
cc-pVQZ-PP	MRCI+Q	2.2039	2.2229	17929.31
cc-pV5Z-PP	MRCI+Q	2.2329	2.5961	20939.44
CBS	MRCI+Q	2.2376	2.6580	21438.71
aug-cc-pV6Z	MRCI+Q	2.1800	2.2687	18293.08
cc-pCVQZ-PP	MRCI+Q	2.2367	2.0543	16569.43
cc-pCV5Z-PP	MRCI+Q	2.2151	2.5829	20832.97
CBS	MRCI+Q	2.2118	2.6715	21547.60
cc-pwCVQZ-PP	MRCI+Q	2.2367	2.0587	16604.92
cc-pwCV5Z-PP	MRCI+Q	2.2118	2.5954	20933.80
CBS	MRCI+Q	2.2080	2.6854	21659.71
aug-pCVQZ-PP	MRCI+Q ^a	2.2354	2.0814	16787.75
aug-pCV5Z-PP	MRCI+Q ^a	2.2332	2.0871	16833.78
CBS	MRCI+Q ^a	2.2322	2.0946	16895.12
aug-pCVQZ-PP	MRCI+Q ^b	2.2273	2.1157	17064.66
aug-pCV5Z-PP	MRCI+Q ^b	2.2204	2.2384	18054.33
CBS	MRCI+Q ^b	2.2187	2.2278	17968.83
cc-pVQZ-PP	CCSD(T), fc ^c	2.3302	2.0311	16382.30
cc-pV5Z-PP	CCSD(T), fc ^c	2.3304	2.0563	16585.56
cc-pCVQZ-PP	CCSD(T), fc ^c	2.3266	2.0494	16529.91
cc-pCV5Z-PP	CCSD(T), fc ^c	2.3280	2.0632	16641.21
cc-pwCVQZ-PP	CCSD(T), fc ^c	2.3279	2.0498	16533.13
cc-pwCV5Z-PP	CCSD(T), fc ^c	2.3282	2.0632	16641.21
cc-pCVQZ-PP	CCSD(T), all ^c	2.2378	2.0298	16371.82
cc-pCV5Z-PP	CCSD(T), all ^c	2.2316	2.0723	16714.61
cc-pwCVQZ-PP	CCSD(T), all ^c	2.2379	2.0355	16417.79
cc-pwCV5Z-PP	CCSD(T), all ^c	2.2327	2.0736	16725.10
aug-cc-pVQZ	RCCSD(T) ^d	2.2400	2.0886	16846.08
aug-cc-pV5Z	MRCI+Q+SOC ^e	2.2417	2.0860	16825.11
Triple-zeta	CIPSI (ECP+CPP) ^f	2.2620	1.9700	15889.49
	Pseudo-potential + LSD ^g	2.4280	2.1000	16938.03
	Pseudo-potential + CISD ^g	2.3707	1.7900	14437.66
Experiment		2.2319 ^h	<2.0271 ⁱ	<16350 ^j
cc-pCVQZ-PP	MRCI+Q (3e) ^k	2.23670	2.0543	16569.43
cc-pCVQZ-PP	MRCI+Q (5e) ^l	2.23725	2.1359	17227.59

^aMRCI+Q, even tempered basis set augmentation functions, present work.

^bMRCI+Q, explicitly energy optimized augmentation functions, present work.

^cCCSD(T), fc and CCSD(T), all : private communication from Peterson (2015).

^dRCCSD(T), Skripnikov and co-workers⁹.

^eMRCI+Q + SOC, Gao *et al*¹².

^fCIPSI Allouche⁸.

^gPseudo-potential + local spin density (LSD)⁶, Pseudo-potential + CISD⁶.

^hExperiment, Ram and Bernath⁵. ⁱExperiment, Kopp *et al*²¹. ^jAssuming Ba(³D₃) limit.

^kMRCI+Q, active 3-electron model, present work. ^lMRCI+Q, active 5-electron model, present work.

close agreement with the experimental r_e value found in the CBS potential supports this choice.

In Table III the results for the equilibrium bond distance r_e and dissociation energy D_e from these CBS limit, MRCI+Q calculations are compared with the coupled cluster approximation CCSD(T)^{40,45–47}, in its various implementations and with other theoretical methods^{8,9,48}. The density functional theory (DFT) work of Wang and Andrews⁴⁸ using a 6-311++G (3*df*, 3*pd*) basis yielded a value of 2.2520 Å and second order Møller Plesset perturbation theory gave 2.2440 Å⁴⁸ respectively for the equilibrium bond distance. Gao *et al*⁴² have conducted calculations for the ground $X^2\Sigma^+$ and the first excited state $A^2\Pi$ of this hydride at the MRCI+Q+SOC level. Their *ab initio* results for the spectroscopic constants r_e (2.2417 Å) and D_e (2.0860 eV) of BaH ($X^2\Sigma^+$) ground state are similar to those obtained from the relativistic - coupled-cluster results⁹ (RCCSDT), respectively 2.24 Å and 2.0840 eV, and in reasonable agreement with the available experimental results⁴⁹. The other *ab initio* results of great accuracy are those using CCSD(T) where the cc-pCV5Z-PP (all electron) result is within 0.02 pm of the experimental value⁵ but if extrapolated to the CBS limit this agreement will be somewhat poorer. Using an aug-cc-pCV*n*Z/CBS MRCI+Q calculation the *ab initio* equilibrium bond distance here is within 0.031 pm of the best spectroscopic value.

III. MODELLING THE GROUND STATE

A. Spectroscopic constants of the ground state

An important requirement is ensuring that the final potential behaves correctly at all interatomic distances, particularly at long-range where dispersion forces are dominant⁵⁰. In atomic units, the asymptotic atom-atom potential has the form⁵¹

$$V(r) \simeq V_\infty - \left(\frac{C_6}{r^6} + \frac{C_8}{r^8} \dots \right) \quad (3)$$

where C_6 , C_8 etc. are the polarizabilities with V_∞ the asymptotic limit (atomic products). r is the atom-atom internuclear separation. The dynamic polarization of the ground state, which allows the computation of the leading C_6 term (148 a.u.), has been calculated⁵² by Derevianko *et al.* To calculate the following C_8 term, the formula derived by Tang⁵³ requires the quadrupole polarizabilities but there are two theoretical values^{54,55} for Ba that produce C_8 values that differ by more than 60%. The smaller value, 11242 a.u., is consistent with the corresponding term calculated⁵⁶ for the neighbouring hydride CsH (11710 a.u.), and is therefore the value recommended at present. There is no theoretical or experimental value at present for C_{10} in BaH so the expansion was truncated at C_8 : the corresponding calculated value⁵⁶ in CsH is 1.194×10^6 a.u.

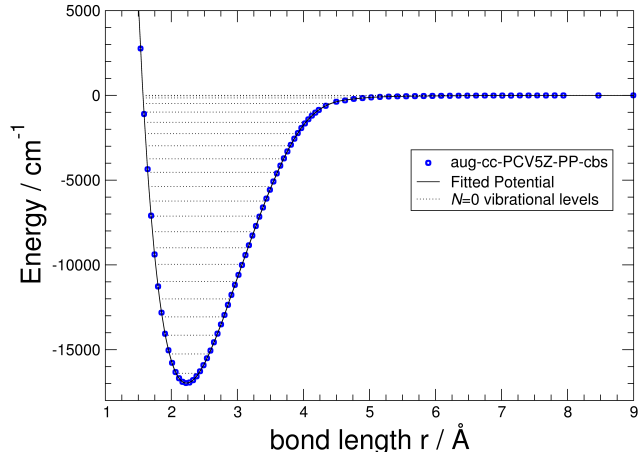


FIG. 3. Analysis of *ab initio* $X^2\Sigma^+$ ground state of BaH using LEVEL⁵⁷. The *ab initio* data was taken with the aug-cc-pCV*n*Z basis sets ($n = 4$ and 5) and extrapolated to the CBS limit. The vibrational levels found in the fit are also presented.

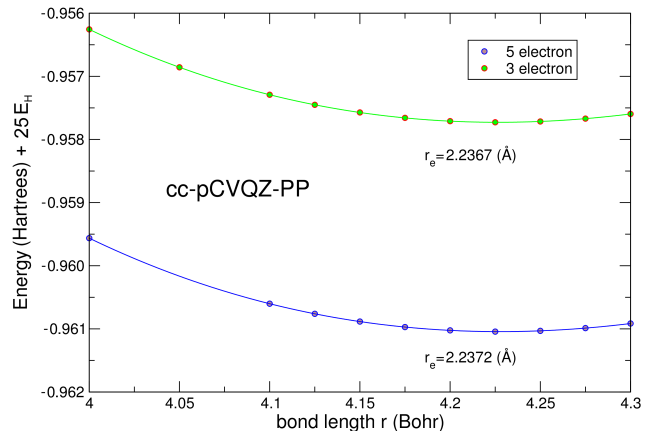


FIG. 4. Comparison of the ground state energy for the BaH molecule in the region of the equilibrium bond distance using both an active 3-electron and 5-electron model in the MRCI+Q approximation. The cc-pCVQZ-PP basis set⁴⁰ is used for both calculations. The absolute energies are adjusted by $25 E_H$.

The LEVEL⁵⁷ program (Version 8.2) was used to calculate the rovibrational levels of the resulting *ab initio* $X^2\Sigma^+$ aug-cc-pCV*n*Z/CBS potential. A smooth potential was produced through interpolation of the *ab initio* points with a 4-point piecewise polynomial (NUSE=4, IR2=1), and extrapolation past $r = 15.88$ Å using a fixed $C_6 = 7.110512 \times 10^5 \text{ cm}^{-1} \text{ Å}^{-6}$ (no C_8 or C_{10}) (ILR=2). Based on this potential the equilibrium bond length and dissociation energy were determined to be

TABLE IV. Vibrational term energies in the $X^2\Sigma^+$ ground state of the BaH molecule. Comparison of the present MRCI+Q results with the aug-cc-pCVnZ-PP even tempered basis set taken to the CBS limit and experimental data. All energies in cm^{-1} .

v''	MRCI	Relative value ^a	Experimental ⁵	RKR ^b	ΔE RKR
0	581.3491	0	0	580.53	0.8191
1	1722.2738	1140.9247	1139.2896	1719.84	2.4338
2	2832.9237	2251.5746	2249.6062	2830.15	2.7737
3	3915.9012	3334.5521	3331.1192	3911.46	4.4412
4	4981.7132	4400.3641		4963.77	17.9432
5	6024.9686	5443.6195		5987.08	37.8886
6	7029.1845	6447.8354		6981.39	47.7945
7	8006.0703	7424.7212		7946.70	59.3703
8	8957.6993	8376.3502		8883.01	74.6893
9	9878.6102	9297.2611		9790.32	88.2902
10	10772.2217	10190.8726		10668.63	103.5917
11	11633.1528	11051.8037			
12	12461.4104	11880.0613			
13	13257.3637	12676.0146			
14	14016.6614	13435.3123			
15	14729.2373	14147.8882			
16	15386.3161	14804.9670			
17	15966.4205	15385.0714			
18	16436.4095	15855.0604			
19	16749.4237	16168.0746			
20	16882.9819	16301.6328			
21	16894.9472	16313.5981			

^a $E(\text{MRCI}) - E(\text{experimental}) = \Delta E (v' - v'') \text{ cm}^{-1}$: (1 - 0) = +1.64; (2 - 1) = +0.33; (3 - 2) = +1.46.

^bBased on experimental data prior⁵⁸ to 1982.

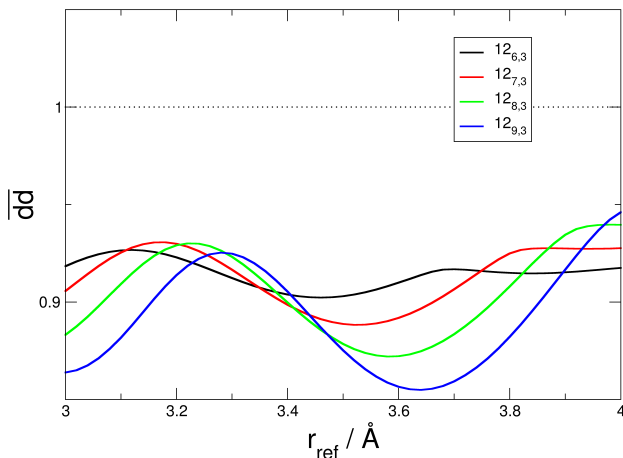


FIG. 5. Tuning r_{ref} to improve the fitting of the *ab initio* $X^2\Sigma^+$ ground state of BaH using *betaFIT*⁵⁹.

2.2322 Å and 16895 cm^{-1} . Twenty-two vibrational levels were predicted for the system, with $v = 21$ lying just 0.2 cm^{-1} below the dissociation limit. Comparison of the relative energies of the first four vibrational levels based

on this potential with experimental values⁵ show good agreement, all within 1.7 cm^{-1} (Table IV). There is a significant jump in the error with respect to the earlier RKR levels at $v = 4$, a result of the lack of experimental data for the higher vibrational levels and consequently the present results are probably more reliable for those missing vibrational levels.

B. 3 electron versus 5 electron MRCI+Q

Though the calculated bond length is only $<0.031 \text{ pm}$ away from the experimental value, another effort was made to explore possible improvements to the accuracy of the *ab initio* potential. In order to quantify the effect of including additional dynamic electron correlation, further MRCI+Q calculations were performed with the cc-pCVQZ-PP basis set⁴⁰ using both 3- and 5-electrons active at the CI stage. From the *ab initio* work shown in Fig. 4 it is found that the active 5-electron model lowers the absolute (total) energy of the ground state minimum for this hydride by just 3 milli-Hartrees (mE_h). The subsequent change in the equilibrium bond distance r_e was also tiny, an increase of 0.055 pm . These very small changes in the total energy and equilibrium distance subsequently justifies the use of the 3-electron model for both the ground and excited states considered as opposed

to the more computationally intensive active 5-electron model.

C. Including spectroscopic data

There is an extensive selection of pair-potentials in the literature to describe the r dependence of the interaction energy in a diatomic molecule (see the supplementary information from Xie *et al* for a comprehensive list⁶⁰ with over a hundred examples). Two of the most successful functions are the Tang-Toennies⁶¹ potential (and its variants) and the Morse-Long-Range⁶² (MLR) function. The *ab initio* data here was fitted to a MLR potential using **betaFIT** (version 2.1)⁵⁹ in order to find an analytical function to express the potential. Prior to fitting, the potential was shifted by 0.03 pm so that the *ab initio* potential minimum was aligned with the experimental r_e value to an accuracy better than 0.01 pm. This simplifies the inclusion of experimental data at a later stage. The MLR potential is described by

$$V_{\text{MLR}}(r) \equiv \mathcal{D}_e \left(1 - \frac{u(r)}{u(r_e)} e^{-\beta(r)y_p^{r_e}(r)} \right)^2 \quad (4)$$

where \mathcal{D}_e is the dissociation energy and $u(r_e)$ is value of $u(r)$ at the equilibrium bond distance.

Both V_{MLR} and $\beta(r)$ are expanded in terms of two internuclear distances r_e and r_{ref} , according to the radial variable

$$y_n^{r_i}(r) = \frac{r^n - r_i^n}{r^n + r_i^n} \quad (5)$$

where $r_i = r_e$ or r_{ref} and the latter is usually greater than or equal to r_e . As the fit is viable for a large range of r_{ref} , it is worth tuning this value to improve the fit (Fig. 5). MLR functions producing local minima were selected as starting points for later fitting to spectral data. Typically, two different values of n are required for an acceptable fit (in the present work, $n = 8$ and 3) in the $\beta(r)$ expansion. The first issue is what to set as the error in the *ab initio* points. Since the vibrational frequencies are calculated to within an average of 2 cm^{-1} the error in each *ab initio* point was initially set rather arbitrarily as 10 cm^{-1} ($5 \times 10^{-5} E_h$). However, Dattani and Le Roy⁶³ have shown that even in the 6e Li_2 molecule a deviation in D_e of up to 68 cm^{-1} still persists in the calculated $b^1\Pi$ state. Therefore, an increased error of 20 cm^{-1} was adopted as a compromise value. The final analytical potential is reported as $\text{MLR}_{p,q}^{r_{ref}}(N_\beta)$, where p and q are the two values of n required and consists of N_β expansion coefficients. A similar⁶⁴ potential (replacing an earlier version⁶⁵ that used only one expansion co-efficient p) has recently been used to describe the ground state of MgH , the only hydride other than H_2 with an experimental dissociation energy determined to sub-wavenumber accuracy. The fitted \mathcal{D}_e is just over 4 cm^{-1} lower than the result from the *ab initio* potential (Table VI), as it was allowed to vary slightly during the fitting process.

The parameters fitted to $\text{MLR}_{8,3}^{3.34}$ (12) from the *ab initio* potential were then transferred to **DPotFit**^{66,67} (version 2.0) and combined with $\text{B}^2\Sigma^+ \rightarrow \text{X}^2\Sigma^+$ emission^{26,28,33} and $\text{X}^2\Sigma^+$ infrared data³⁵. The earlier emission data was quoted to 0.01 cm^{-1} while the stated resolution of the infrared data was 0.005 cm^{-1} .

While $r_{ref} = 3.34 \text{ \AA}$ does not correspond to a local minimum in Fig. 5, those MLRs obtained from the local minima in **betaFIT** were not found to be as successful. $p = 8, q = 3$ were selected as the best parameters after screening other combinations. As **DPotFit** utilizes a dimensionless root-mean-square-deviation (\overline{dd}) as its means of determining how closely a model matches the observed data, it is crucial that a reasonable assessment of the uncertainty in the observable data is made.

$$\overline{dd} = \sqrt{\frac{1}{N_{\text{data}}} \sum_{i=1}^{N_{\text{data}}} \left(\frac{E_{\text{calc}}(i) - E_{\text{obs}}(i)}{u_{\text{obs}}(i)} \right)^2} \quad (6)$$

Thus, as the uncertainty in the *ab initio* E_{obs} was set to 20 cm^{-1} , deviations from the fitted MLR do not lead to a large increase in the \overline{dd} . At the chosen r_{ref} the \overline{dd} between the $\text{MLR}_{8,3}^{3.34}$ (12) potential fitted by **betaFIT** and the *ab initio* points was only 0.4570 representing a close fit within the selected uncertainty. By contrast the original emission data was quoted to much higher accuracy, so any deviations between the model and the spectral measurements can lead to a significant increase (left hand data, Table VI) in \overline{dd} . Due to the arbitrary nature of the uncertainty assignment in the *ab initio* data, the associated \overline{dd} should not be compared directly to the \overline{dd} in fits to experimental data.

As **DPotFit** tries to fit to very accurate spectroscopic data, the initial uncertainty in the fit is very high. Allowing β parameters to become fitted parameters produces a final potential which matches the experimental data much more closely than the *ab initio* potential alone. During the fitting, both C_6 and C_8 were fixed at the recommended theoretical values, and were incorporated as the long range tail of the MLR potential with Douketis-type damping⁶⁸ with $s = -1$. Additionally, the effect of spin rotation coupling is incorporated through a modification to the MLR potential⁶⁷ using the expansion coefficients listed in Table VII.

As the considered spectral data covers a range of isotopomers of BaH (electronic transitions of ^{138}BaH and ^{138}BaD ; infrared transitions of ^{138}BaH , ^{137}BaH , ^{136}BaH , ^{135}BaH), all of which have very small values of reduced mass, it is valuable to consider the impact of the Born-Oppenheimer breakdown (BOB)⁶⁹ corrections. **DPotFit** incorporates BOB corrections through the atom-dependant potential, with the effects parametrised within the radial strength functions:

$$\tilde{S}_{\text{ad}}^{\text{A}}(r) = y_{p_{\text{ad}}}^{eq}(r) u_{\infty}^{\text{A}} + [1 - y_{p_{\text{ad}}}^{eq}(r)] \sum_{i=0}^{N_{\text{ad}}^{\text{A}}} u_i^{\text{A}} y_{p_{\text{ad}}}^{eq}(r)^i \quad (7)$$

TABLE V. Summary of the spectral data used when fitting with **DPotFit**. A total of 1769 B²Σ-X²Σ transition and 409 X²Σ⁺ IR emission lines were incorporated.

Year	Transition	Isotope	$v' - v'' (J_{max})$	Lines	Unc / cm ⁻¹
1933 ²⁶	B ² Σ ⁺ → X ² Σ ⁺	¹³⁸ Ba ¹ H	0-0 (37.5)	112	0.01
1935 ²⁸	B ² Σ ⁺ → X ² Σ ⁺	¹³⁸ Ba ¹ H	1-0 (41.5)	142	0.01
			1-1 (31.5)	106	0.01
			2-1 (37.5)	126	0.01
1966 ³³	B ² Σ ⁺ ← X ² Σ ⁺	¹³⁸ Ba ² H	0-0 (52.5)	197	0.01
			1-0 (47.5)	177	0.01
			0-1 (42.5)	146	0.01
			1-1 (50.5)	179	0.01
			2-1 (46.5)	162	0.01
			1-2 (33.5)	94	0.01
			2-2 (44.5)	142	0.01
			3-2 (39.5)	125	0.01
			3-3 (29.5)	61	0.01
1993 ³⁵	IR	¹³⁸ Ba ¹ H	1-0 (28.5)	94	0.005
			2-1 (20.5)	80	0.005
			3-2 (29.5)	77	0.005
		¹³⁷ Ba ¹ H	1-0 (22.5)	59	0.005
			¹³⁶ Ba ¹ H	1-0 (22.5)	59
		¹³⁵ Ba ¹ H	1-0 (19.5)	40	0.005

TABLE VI. The MLR_{*p,q*}^{*r,ref*}(*N*_β) potential parameters obtained through a fit to the *ab initio* potential, and after initial optimization with spectral data using **DPotFit**. All energies in cm⁻¹.

MLR _{8,3} ^{3,34} (12), <i>ab initio</i> only				MLR _{8,3} ^{3,34} (12), <i>ab initio</i> + spectra			
\mathfrak{D}_e 16891.5947		r_e 2.2319 Å		\mathfrak{D}_e 16841.8651		r_e 2.2318 Å	
\overline{dd} 266.447				\overline{dd} 6.083			
β_0 0.114040	β_7 -87.820760	β_0 0.096691	β_7 -86.606654	β_1 -7.619529	β_8 -171.874803	β_1 -7.616896	β_8 -154.070717
β_2 -17.121381	β_9 -5.387603	β_2 -16.467554	β_9 34.3428882	β_3 -19.233860	β_{10} 256.820563	β_3 -16.902752	β_{10} 324.143391
β_4 3.673494	β_{11} 260.900999	β_4 6.565879	β_{11} 334.502110	β_5 44.305094	β_{12} 83.391642	β_5 44.183256	β_{12} 116.057107
β_6 31.801460		β_6 28.715007					

$$\tilde{R}_{na}^A(r) = y_{p_{na}}^{eq}(r) t_{\infty}^A + [1 - y_{p_{na}}^{eq}(r)] \sum_{i=0}^{N_{na}^A} t_i^A y_{p_{ad}}^{eq}(r)^i \quad (8)$$

Where $\tilde{S}_{ad}^A(r)$ is the atom-dependant adiabatic BOB radial strength function and $\tilde{R}_{na}^A(r)$ the non-adiabatic BOB radial strength function. Incorporating fitted terms (Table VII) for $N_{ad} = N_{na} = 2$ along with fitted MLR parameters (Table VI) while keeping r_e fixed at 2.2319 Å produced an MLR potential with $\overline{dd} = 6.143$. Allowing r_e to also be a fitted parameter lowered \mathfrak{D}_e by nearly 50 cm⁻¹ but further reduced \overline{dd} to 6.083. While substantially higher than what would usually be deemed a “good” fit⁶⁷ ($\overline{dd} < 1$), comparison with results from the most recent study⁵ of the E(2Π) → X(2Σ⁺) transition, a data set not used in the **DPotFit** analysis, highlights the

much improved agreement with the experimental observations (Table VIII) than the raw *ab initio* results from Table IV.

In addition, a number of further details were evident while developing the hybrid potential. The experimental values³⁵ for the spin-rotation constant $\gamma(v)$ follow a very clear v dependence^{70,71} (Fig. 6) that can be modelled as a simple Taylor (linear) expansion:

$$\gamma(v) = \gamma_0 + \gamma_1 \left(v + \frac{1}{2} \right) \quad (9)$$

with $\gamma_0 = 0.19456$ cm⁻¹ and $\gamma_1 = -4.9813 \times 10^{-3}$ cm⁻¹. Finally, the experimental dissociation energy quoted in the literature has its origin in the sudden onset of rapid predissociation in the C²Σ⁺ $v' = 1$, $N' = 10$ rovibronic

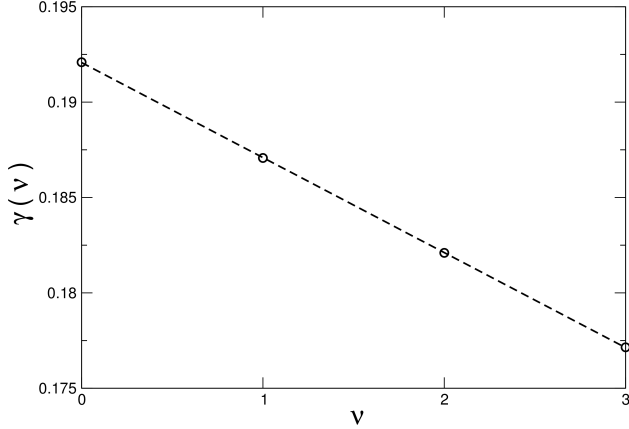


FIG. 6. The v dependence of the experimental spin-rotation constants γ from the experimental work³⁵ of Walker, Hedderich and Bernath.

TABLE VII. Additional parameters defining the $^2\Sigma^+$ spin-rotation coupling and the BOB corrections in the final MLR potential, obtained after initial optimisation with spectral data using DPotFit.

MLR $_{8,3}^{3,34}(12)$, Additional parameters			
q_0^Σ	3		
w_0^Σ	0.058666		
w_1^Σ	-0.034468		
w_2^Σ	-0.015660		
p_{ad}	6		
u_0^{Ba}	14.158630	u_0^H	-81.921108
u_1^{Ba}	-106.246129	u_1^H	244.705054
u_2^{Ba}	-3.266579	u_2^H	-25.518624
u_∞^{Ba}	0.000000	u_∞^H	0.000000
p_{na}	3		
q_{na}	3		
t_0^{Ba}	-0.007379	t_0^H	0.007367
t_1^{Ba}	0.003445	t_1^H	0.000210
t_2^{Ba}	-0.015764	t_2^H	-0.049889
t_∞^{Ba}	0.000000	t_∞^H	0.000000

level. This level lies $25942.6 \pm 0.5 \text{ cm}^{-1}$ above the $X^2\Sigma^+$ minimum. Assuming that this indicates the dissociation limit of the (diabatic) $D^2\Sigma^+$ potential lies above $C^2\Sigma^+$ $v' = 1$, $N' = 9$ ($25874.6 \pm 0.3 \text{ cm}^{-1}$) and identifying the asymptote as belonging to $Ba(^3D_1)$ and not $Ba(^3D_3)$, this would fix the dissociation energy D_e of the ground state between 16842.6 cm^{-1} and 16910.6 cm^{-1} which is consistent with the present *ab initio* value and other recent theoretical⁹ results, while the DPotFit result is within 1 cm^{-1} of the lower limit. It is therefore tentatively suggested that the correct dissociation limit for the $D^2\Sigma^+$

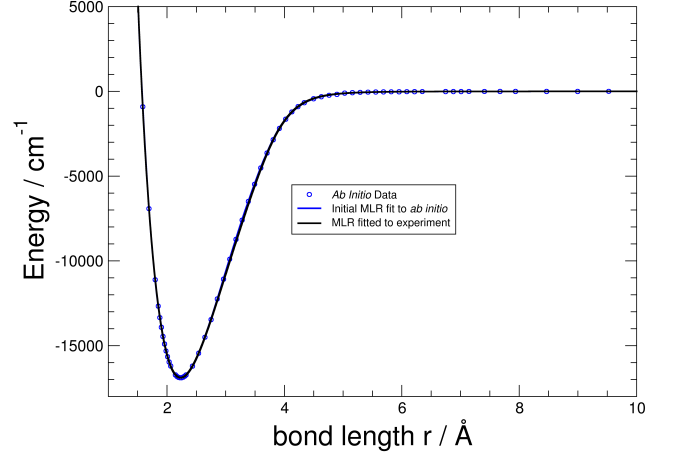


FIG. 7. MLR $_{8,3}^{3,34}(12)$ fit to *ab initio* data points, and final MLR $_{8,3}^{3,34}(12)$ fit to experimental data.

state is actually $Ba(^3D_1) + H(^2S_{1/2})$ and at long range ought to be labelled $D_{\frac{1}{2}}^1(1)$ in Hund's case (c).

D. Excited states

Extending the *ab initio* study to excited states, the lowest energy $^2\Pi$ state was calculated using the even tempered augmented cc-pCV5Z-PP basis set⁴⁰. Despite being carried out with a CASSCF calculation including $5A_1$, $5B_1$ and $5A_2$ states and the MRCI being carried out over $5B_1$ states, the resulting potential has an r_e of 2.2698 \AA , within 0.38 pm of the best experimental value from Barrow (quoted in Allouche⁸ *et al.*). The calculated difference in $X^2\Sigma^+$ and $A^2\Pi$ bond lengths is therefore $\Delta r_e = 3.97 \text{ pm}$ compared to the experimental difference of 4.16 pm , a discrepancy of just 2 m\AA . Of course, for a truly faithful reproduction of the $A^2\Pi$ state not only must spin-orbit coupling be included in the calculation, but also the angular momentum coupling with other electronic states. However, for FC factors the fact that Δr_e is so close to experiment is reassuring and small energy shifts in general do not have a large effect.

The two potentials were then used to obtain FC factors between the $X^2\Sigma^+$ and $A^2\Pi$ vibronic states using LEVEL. The highly diagonal nature of the $A^2\Pi \leftarrow X^2\Sigma^+$ transition is clear when the wavefunctions from both states are compared as in Fig. 8. The diagonal FC factor f_{00} is almost identical to that found in the earlier study by Lane¹ using the larger ECP and a much smaller triple zeta quality basis set, though the agreement reduces with each increase in vibrational quantum number (by f_{33} the difference is 5.8%, compared to 0.1% for f_{00}). Using the revised dissociation energy D_e of the ground state ($< 16910.6 \pm 0.5 \text{ cm}^{-1}$), the $^3D - ^1S$ separation in bar-

TABLE VIII. Vibrational term energies in the $X^2\Sigma^+$ ground state of the BaH molecule using DPotFit. Comparison of the vibrational levels from the present combined *ab initio*/spectroscopic potential and experimental⁵ data independent of fit. All energies in cm^{-1} .

v	Experiment (Ram <i>et al</i>)	DPotFit ^a r_e fix	ΔE r_e fix	DPotFit ^b r_e fit	ΔE r_e fit
0	0.0000	0.0000	0.0000	0.0000	0.0000
1	1139.2896	1139.2884	-0.0012	1139.2897	0.0001
2	2249.6062	2249.6084	-0.0022	2249.6078	-0.0016
3	3331.1192	3331.1212	-0.0020	3331.1234	-0.0042

^a Zero Point Energy = 580.6050 cm^{-1}

^b Zero Point Energy = 580.5910 cm^{-1}

ium (9372 cm^{-1}), the Term energy of the minimum of the $A^2\Pi$ potential (excluding spin-orbit separation) from Barrow⁷² and co-workers and finally the $X^2\Sigma^+$ zero point energy, the experimental dissociation energy D_e of the $A^2\Pi$ state is $< 16001.3 \pm 2.0 \text{ cm}^{-1}$ which is in good agreement with our calculated value of 16076.75 cm^{-1} . This is further support for our proposed revision of the experimental value for the BaH $X^2\Sigma^+$ dissociation energy D_e to $< 16910.6 \pm 0.5 \text{ cm}^{-1}$.

Using the same basis set, *ab initio* calculations were performed in the MRCI+Q approximation for five states of each of the 2A_1 , 2B_1 and 2A_2 symmetries for bond length out to $40 a_0$. The results from all these calculations are presented in Fig. 9. The 2A_1 states are the most common symmetry at lower energies and therefore valence states dominate in Fig. 9. Comparing to the previous AV6Z calculation, the less diffuse nature of the largest Gaussian functions in our adopted aug-pCVnZ-PP basis sets has resulted in the greater weighting of valence states over Rydbergs and so the $C^2\Sigma^+$ state has disappeared. To describe the Rydberg character of the $^2\Sigma^+$ states, it's necessary to expand the active space in the MRCI+Q calculations to at least $(8a_1, 5b_1, 3b_2, 2_2)$.

IV. SUMMARY AND CONCLUSION

In this paper we have attempted to develop a reliable potential energy curve for the $X^2\Sigma^+$ state of the BaH radical. Encouraged by the close agreement in the literature between relativistic and non-relativistic *ab initio* calculations, we have used the MRCI+Q method to determine the shape of the $X^2\Sigma^+$ potential and the dissociation energy. With an even-tempered augmented cc-pCVnZ-PP basis set taken to the CBS limit, we have calculated the equilibrium bond length to within 0.031 pm of the experimental value and of comparable accuracy

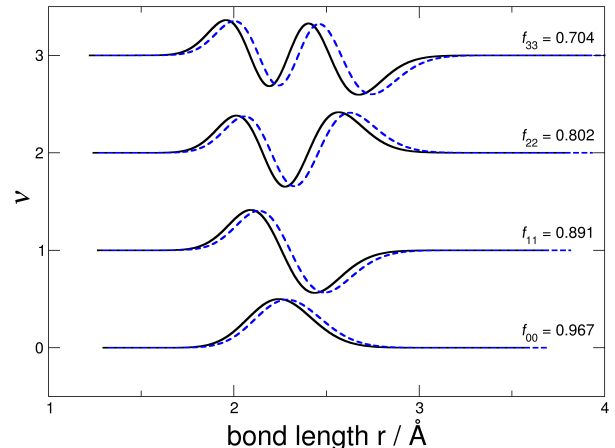


FIG. 8. The almost identical first four vibrational wavefunctions in the X and A states of BaH. The larger equilibrium bond length displaces the excited state slightly but the overlap is sufficient to ensure diagonal Franck-Condon factors close to 1. Also labelled are the diagonal Franck-Condon (FC) factors $f_{v_i v_i}$.

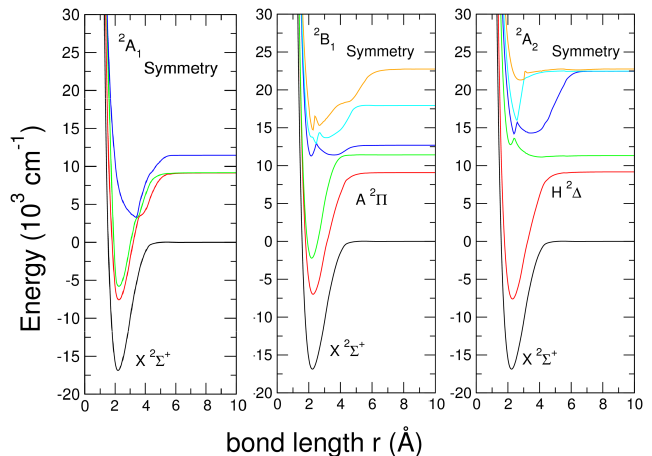


FIG. 9. Low lying states of BaH using an active 3-electron model in the MRCI+Q approximation. The even tempered aug-cc-pCV5Z-PP basis set is used for the calculations.

to the more trusted CCSD(T) technique. While the ten $5s5p6s$ electrons from barium are necessary to calculate the static correlation energy, only the valence $6s$ electrons are needed to cover the majority of the dynamic correlation. The computed dissociation energy (16895.12 cm^{-1}) is in good agreement with other theoretical values suggesting a revision of the experimental dissociation energy to $D_e < 16910.6 \text{ cm}^{-1}$. The calculated dissociation energy of the excited $A^2\Pi$ state (16076.75 cm^{-1}) is also

consistent with this experimental value. The vibrational levels of the *ab initio* $X^2\Sigma^+$ potential achieve an average agreement of just over 1 cm^{-1} with the best experimental values. Refining the potential with experimental data using DPotFit improves the agreement to better than 0.005 cm^{-1} for the lowest vibrational levels.

ACKNOWLEDGMENTS

I. C. L. thanks the Leverhulme Trust for financial support, a PDRA fellowship for B. M. M. and a Ph D studentship for K. M. under Research Grant RPG-2014-212. We would like to thank Professor K. Peterson for providing the explicitly optimized augmented functions for the barium atom for his cc-pCVnZ-PP basis sets and for many helpful discussions regarding this *ab initio* work. Grants of computational time at the National Energy Research Scientific Computing (NERSC) Center in Oakland, CA, USA and at the High Performance Computing Center Stuttgart (HLRS) of the University of Stuttgart, Stuttgart, Germany, where some of these computations were performed, are gratefully acknowledged.

- ¹I. C. Lane, Phys. Rev. A **92**, 022511 (2015).
- ²H. J. Werner and P. J. Knowles, Chem. Phys. Lett. **115**, 259 (1985).
- ³H. J. Werner and P. J. Knowles, J. Chem. Phys. **89**, 5803 (1988).
- ⁴M. G. Tarallo, G. Z. Iwata, and T. Zelevinsky, Phys. Rev. A **93**, 032509 (2016).
- ⁵R. S. Ram and P. F. Bernath, J. Mol. Spec. **283**, 18 (2013).
- ⁶P. Fuentealba, O. Reyes, H. Stoll, and H. Preuss, J. Chem. Phys. **87**, 5338 (1987).
- ⁷M. Kaupp, P. Schleyer, H. Stoll, and H. Preuss, J. Chem. Phys. **94**, 1360 (1991).
- ⁸A. R. Allouche, G. Nicolas, J. C. Barthelat, and F. Spiegelmann, J. Chem. Phys. **96**, 7646 (1992).
- ⁹L. V. Skripnikov, N. S. Mosyagin, and A. V. Titov, Chem. Phys. Lett. **555**, 79 (2013).
- ¹⁰V. A. Kostelevy and A. J. Vargas, Phys. Rev. D **92**, 056002 (2015).
- ¹¹W. Ubachs, J. Koelemeij, K. Eikema, and E. Salumbides, J. Mol. Spectro. **320**, 1 (2016).
- ¹²J. S. Rigden, Hist. Stud. Phys. Sci. **13**, 335 (1983).
- ¹³H. Kragh, Hist. Stud. Phys. Sci. **15**, 67 (1985).
- ¹⁴B. Cagnac, M. D. Plimmer, L. Julien, and F. Biraben, Rep. Prog. Phys. **57**, 853 (1994).
- ¹⁵S. G. Karshenboim, Phys. Rev. A **91**, 012515 (2015).
- ¹⁶J. Koput, J. Chem. Phys. **135**, 244308 (2011).
- ¹⁷N. S. Dattani, J. Mol. Spectrosc. **311**, 76 (2015).
- ¹⁸H.-J. Werner, P. J. Knowles, R. Lindh, F. R. Manby, and M. S. *et. al.*, "MOLPRO 2010, <http://www.molpro.net>," .
- ¹⁹R. J. Gdanitz and R. Ahlrichs, Chem. Phys. Lett. **143**, 413 (1988).
- ²⁰R. J. Le Roy, D. R. Appadoo, R. Colin, and P. F. Bernath, J. Mol. Spectrosc. **236**, 178 (2006).
- ²¹I. Kopp, N. Åslund, G. Edvinsson, and B. Lindgren, Ark. Fysik. **30**, 321 (1966).
- ²²A. Eagle, Astrophys. J. **30**, 231 (1909).
- ²³A. Schaafsma, Z. Phys. **74**, 254 (1932).
- ²⁴W. R. Fredrickson and W. W. Watson, Phys. Rev. **39**, 753 (1932).
- ²⁵G. Funke, Z. Phys. **84**, 610 (1933).
- ²⁶W. W. Watson, Phys. Rev. **43**, 9 (1933).
- ²⁷W. W. Watson, Phys. Rev. **47**, 213 (1935).
- ²⁸P. G. Koontz and W. W. Watson, Phys. Rev. **48**, 937 (1935).
- ²⁹G. Fabre, A. El-Hachimi, R. Stringat, C. Effantin, A. Bernard, J. DIncan, and J. Vergès, J. Phys. B: At. Mol. Phys. **20**, 1933 (1987).
- ³⁰B. Grunström, Z. Phys. **99**, 595 (1936).
- ³¹G. W. Funke and B. Grunström, Z. Phys. **100**, 293 (1936).
- ³²G. Edvinsson, I. Kopp, B. Lindgren, and N. Åslund, Ark. Fysik. **25**, 95 (1963).
- ³³I. Kopp and R. Wirhed, Ark. Fysik. **32**, 307 (1966).
- ³⁴I. Kopp, M. Kronekvist, and A. Guntzsch, Ark. Fysik. **32**, 371 (1966).
- ³⁵K. A. Walker, H. G. Hedderich, and P. F. Bernath, Mol. Phys. **78**, 577 (1993).
- ³⁶P. Siegbahn, A. Heiberg, B. Roos, and B. Levy, Phys. Scr. **21**, 323 (1980).
- ³⁷H. J. Werner and P. J. Knowles, J. Chem. Phys. **82**, 5053 (1985).
- ³⁸L. Meissner, Chem. Phys. Lett. **146**, 204 (1988).
- ³⁹S. Langhoff and E. R. Davidson, Int. J. Quantum Chemistry **8**, 61 (1974).
- ⁴⁰K. Peterson, "private communication, all the basis sets are available from the Peterson group website, <http://tyr0.chem.wsu.edu/~kipeters/basis.html> save aug-cc-pCVnZ-PP," (2015).
- ⁴¹I. S. Lim, H. Stoll, and P. Schwerdtfeger, J. Chem. Phys. **124**, 034107 (2006).
- ⁴²Y. Gao and T. Gao, Phys. Rev. A **90**, 052505 (2014).
- ⁴³F. Jensen, Theo. Chem. Acc. **113**, 267 (2005).
- ⁴⁴A. Karton and J. M. L. Martin, Theo. Chem. Acc. **115**, 330 (2006).
- ⁴⁵J. Čížek, J. Chem. Phys. **45**, 4256 (1966).
- ⁴⁶G. D. Purvis III and R. J. Barlett, J. Chem. Phys. **76**, 1910 (1982).
- ⁴⁷J. D. Watts, J. Gauss, and R. J. Barlett, J. Chem. Phys. **98**, 8718 (1993).
- ⁴⁸X. Wang and L. Andrews, J. Phys. Chem. A **108**, 11500 (2004).
- ⁴⁹P. J. Linstrom and W. G. Mallard, "NIST Chemistry WebBook NIST Standard Reference Database Number 69," National Institute of Standards and Technology, Gaithersburg, MD, USA, <http://www.webbook.nist.gov> (2005).
- ⁵⁰J. Mitroy, M. S. Safronova, and C. W. Clark, J. Phys. B: At. Mol. Opt. Phys. **43**, 202001 (2010).
- ⁵¹R. Côte and A. Dalgarno, Phys. Rev **62**, 012709 (2000).
- ⁵²A. Derevianko, S. G. Porsev, and J. F. Babb, Atomic Data and Nuclear Data Tables **96**, 323 (2010).
- ⁵³K. T. Tang, Phys. Rev. **177**, 108 (1969).
- ⁵⁴S. H. Patil, Eur. Phys. J. D **10**, 341 (2000).
- ⁵⁵S. G. Porsev and A. Derevianko, JETP, **102**, 195 (2006).
- ⁵⁶S. H. Patil and K. T. Tang, J. Chem. Phys. **106**, 2298 (1997).
- ⁵⁷R. J. Le Roy, LEVEL 8.2 University of Waterloo Chemical Physics Research Report CP-668 (2014).
- ⁵⁸M. Ramanaish and S. Lakishman, Physica C **113**, 263 (1982).
- ⁵⁹R. J. Le Roy, betaFIT University of Waterloo Chemical Physics Research Report CP-666 (2013).
- ⁶⁰J. C. Xie, S. K. Mishra, T. Kar, and R.-H. Xie, Chem. Phys. Lett. **605**, 137 (2014).
- ⁶¹K. T. Tang and J. P. Toennies, J. Chem. Phys. **80**, 3726 (1984).
- ⁶²R. J. Le Roy, Y. Y. Huang, and C. Jary, J. Chem. Phys. **125**, 164310 (2006).
- ⁶³N. S. Dattani and R. J. Le Roy, ArXiv , 1508.07184 (2015).
- ⁶⁴R. Henderson, A. Shayesteh, J. Tao, C. Haugen, P. Bernath, and R. Le Roy, J. Phys. Chem. A **117**, 133373 (2013).
- ⁶⁵A. Shayesteh, R. D. E. Henderson, R. J. Le Roy, and P. F. Bernath, J. Phys. Chem. A **111**, 12495 (2007).
- ⁶⁶R. J. Le Roy, N. S. Dattani, J. A. Coxon, A. J. Ross, P. Crozet, and C. Linton, J. Chem. Phys. **131**, 204309 (2009).
- ⁶⁷R. J. Le Roy, DPotFit University of Waterloo Chemical Physics Research Report CP-667 (2013).
- ⁶⁸C. Douketis, G. Scoles, S. Marchetti, M. Zen, and A. J. Thakkar, J. Chem. Phys. **76**, 3057 (1982).
- ⁶⁹R. J. Le Roy and Y. Huang, Journal of Molecular Structure (Theochem) **591**, 175 (2002).

⁷⁰J. M. Brown and J. K. G. Watson, *J. Mol. Spectrosc.* **65**, 65 (1977).

⁷¹M. Semczuk, X. Li, W. Gunton, M. Haw, N. S. Dattani, J. Witz, A. K. Mills, D. J. Jones, and K. W. Madison, *Phys. Rev. A* , 052505 (2013).

⁷²A. Bernard, C. Effantin, J. d'Incan, G. Fabre, R. Stringat, and R. F. Barrow, *Mol. Phys.* **67**, 1 (1989).